PHYSICAL REVIEW B **89**, 201114(R) (2014)

Bilayer splitting and wave functions symmetry in $Sr_3Ir_2O_7$

L. Moreschini,[1,*] S. Moser,[2] A. Ebrahimi,[2] B. Dalla Piazza,[2] K. S. Kim,[1,3,4] S. Boseggia,[5,6] D. F. McMorrow,[5] H. M. Rønnow,[2] J. Chang,[2] D. Prabhakaran,[7] A. T. Boothroyd,[7] E. Rotenberg,[1] A. Bostwick,[1] and M. Grioni[2]

[1]*Advanced Light Source (ALS), Lawrence Berkeley National Laboratory, Berkeley, California 94720, USA*

[2]*Institute of Condensed Matter Physics (ICMP), Ecole Polytechnique Fédérale de Lausanne (EPFL), CH-1015 Lausanne, Switzerland*

[3]*Department of Physics, Pohang University of Science and Technology, Pohang 790-784, Korea*

[4]*Center for Artificial Low Dimensional Electronic Systems, Institute for Basic Science, Pohang 790-784, Korea*

[5]*London Centre for Nanotechnology, University College London, London WC1E 6BT, United Kingdom*

[6]*Diamond Light Source Ltd., Harwell Science and Innovation Campus, Didcot, Oxfordshire OX11 0DE, United Kingdom*

[7]*Clarendon Laboratory, Department of Physics, University of Oxford, Parks Road, Oxford OX1 3PU, United Kingdom*

(Received 23 February 2014; revised manuscript received 2 May 2014; published 23 May 2014)

The influence of dimensionality on the electronic properties of layered perovskite materials remains an outstanding issue. We address it here for $Sr_3Ir_2O_7$, the bilayer compound of the iridate $Sr_{n+1}Ir_nO_{3n+1}$ series. By angle-resolved photoemission spectroscopy we show that in this material the interlayer coupling is large and that the intercell coupling is, conversely, negligible. From a detailed mapping of the bilayer splitting, and from the intensity modulation of the bonding and antibonding bands with photon energy, we establish differences and similarities with the prominent case of the bilayer superconducting cuprates.

DOI: 10.1103/PhysRevB.89.201114 PACS number(s): 71.20.−b, 71.30.+h, 79.60.−i

Iridium oxides are generating increasing attention [1–13]. In these materials, the entanglement of the spin and orbital degrees of freedom induces a reorganization of the electronic energy levels, described by an effective total angular momentum J_{eff}. This is different from the case of $3d$ and $4d$ oxides, governed by Coulomb interactions and, respectively, Hund's coupling [14]. The interaction between such composite moments strongly depends on the symmetry of the Ir-O covalent bonds [10,15]. In spite of such differences, iridates built from corner sharing IrO_6 octahedra, such as Sr_2IrO_4, show surprising analogies with the isostructural cuprate compounds, namely, a single band at the Fermi level [2] and a similar magnetic structure [1,4,6]. This motivates a search for connections between iridates and cuprates and, quite naturally, most studies have been performed on the Ruddlesden-Popper series $Sr_{n+1}Ir_nO_{3n+1}$, which shows a close similarity with the layered cuprates housing high-temperature superconductivity.

Experimental efforts have been so far oriented to the stoichiometric "parent compounds", and to the role of structural distortions and of dimensionality in determining both the electronic and the magnetic properties. Insight into the former is gained by substituting Sr with, e.g., Ba, which enhances the tetragonal distortion and prevents the rotation of the IrO_6 octahedra [16]. The effect of dimensionality can be assessed by comparing the compounds of the series from n=1, the two-dimensional (2D) limit, to $n \to \infty$, the three-dimensional (3D) one. Early optical data showed an evolution from a Mott insulator (Sr_2IrO_4) to a correlated metal ($SrIrO_3$), which was attributed to interlayer coupling and a consequent increase of the bandwidth W [3]. A similar evolution is observed in cuprates where, e.g., La_2CuO_4 is a charge transfer insulator [17], whereas $LaCuO_3$ is a poor metal [18,19].

In between these two extremes, $Sr_3Ir_2O_7$ is notable, as a small electronic gap seems to indicate that it lies very close to the critical point marking the metal-to-insulator transition. Its band structure has been mapped for the first time with laser-based angle-resolved photoemission spectroscopy (ARPES) [20], and refined more recently [21,22]. Reference [21] suggests a polaronic ground state with a vanishing quasiparticle pole close to the Fermi level, another possible similarity to the cuprates [23]. Alternatively, Ref. [22] ascribes the reduced gap to the intercell coupling, which would cause a sizable dispersion in the direction perpendicular to the IrO layers and mark a departure from the 2D physics already for $n = 2$. Our results suggest a different scenario. We measure a bilayer splitting between bonding and antibonding bands as large as 0.2 eV, which indicates that the interlayer coupling cannot be treated simply as a perturbative term to the electronic structure of the monolayer counterpart. From the intensity modulation of these states with photon energy, we infer the reflection symmetry properties of the corresponding wave functions. We find that the lowest energy state is antisymmetric, opposite to the much studied case of the bilayer cuprates.

Single crystals of $Sr_3Ir_2O_7$ were grown using the self-flux technique, as described elsewhere [24], and characterized by magnetization measurements, x-ray diffraction, x-ray resonant magnetic scattering, and resonant inelastic scattering. All the ARPES data were measured at beamline 7.0.1 of the Advanced Light Source with a Scienta analyzer, and the momentum and energy resolution were 0.1° and 30 meV at $h\nu = 100$ eV, respectively. The light was linearly polarized in the horizontal plane containing the k_x axis of the sample and the analyzer slits (p scattering geometry), and the angular scans were obtained by rotating the sample about k_x, in steps of k_y. The measurements were performed at $T = 30$ K and no charging effects were observed at this temperature.

Figure 1 shows an overview of the band topology of $Sr_3Ir_2O_7$. The crystal structure has recently been refined from tetragonal to orthorhombic [25] but, as common practice in these layered iridates, we discuss the data with reference to a square surface Brillouin zone (BZ), as shown in Fig. 1(a). As we will show later, this choice is certainly justified for

*lmoreschini@lbl.gov

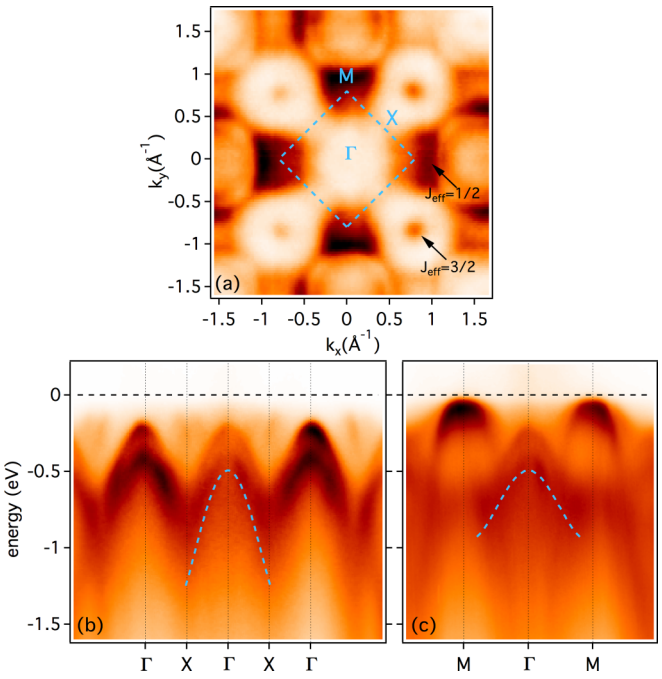

FIG. 1. (Color online) (a) ARPES constant energy cut taken at $E = -180$ meV, near the top of the $J_{\rm eff} = 3/2$ states. The square indicates the surface BZ, determined by the in-plane rotation of the IrO_6 octahedra and the G-type antiferromagnetic ordering. The characteristic contours of the distinct $J_{\rm eff}$ bands are indicated by arrows. (b) and (c) show the band dispersion along the two high-symmetry directions through Γ. Note in (b) the intensity modulation due to the folding potential generated by the structural distortion. The dashed curves outline the dispersion along the same directions for the monolayer compound Sr_2IrO_4, as reported in Ref. [2]. The relevant dimensions are $\overline{\Gamma M} = 0.78$ Å^{-1} and $\overline{\Gamma X} = 0.55$ Å^{-1}.

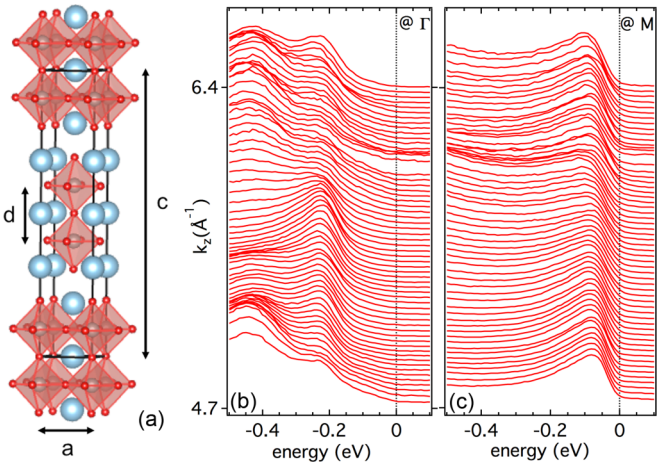

FIG. 2. (Color online) (a) The crystal structure of $Sr_3Ir_2O_7$, where the IrO_6 octahedra are colored and the large spheres indicate Sr atoms; a and c are the lattice constants parallel and normal to the Ir-O layers, respectively, and d is the bilayer spacing. (b) and (c) show stacks of spectra measured for varying photon energy at Γ and M, where the intensity is normalized to the lowest binding energy peak, at -0.23 and -0.09 eV, respectively. The slight irregularity in the measured intensity around $k_z = 6$ Å^{-1} is due to the Sr $3d$ doublet generated by second order radiation from the monochromator. The k_z values are calculated assuming an inner potential $V_0 = 10$ eV. Note that due to the lack of a measurable k_z periodicity a precise extraction of V_0 is not possible. However, it can be approximately set to 10 eV through analysis of the photoemission intensity modulation (see text).

our bilayer compound. The dispersion shown in Figs. 1(b) and 1(c) is in general agreement with previous reports [20–22]. The intensity in the first eV below the Fermi level is due to two manifolds of holelike bands. The lowest energy state has maximum at -90 meV, i.e., 90 meV below the Fermi level E_F, at the M point. A second manifold has maximum at the Γ point at -0.23 eV. The experimental band dispersion shows marked similarities with that of Sr_2IrO_4, where the states are assigned to $J_{\rm eff} = 1/2$ and $J_{\rm eff} = 3/2$ character as indicated by the arrows in Fig. 1(a), but each band is further split into a bonding and an antibonding branch. While significant hybridization between these two manifolds is expected here, we keep the same labeling for simplicity. Such assignment of the bands to a specific $J_{\rm eff}$ character remains accurate near the Γ and M high-symmetry points, where hybridization is negligible [26]. The dashed curves in Figs. 1(b) and 1(c) indicate the measured dispersion of the $J_{\rm eff} = 3/2$ band in Sr_2IrO_4 [2]. As noted in a recent comparative ARPES study [22], the monolayer bands are clearly not in the center of the split states of the bilayer, as expected if the interaction between states on the two Ir-O planes were small with respect to the other relevant energy scales.

It was argued [22] that this energy shift could be ascribed to the interaction between two adjacent unit cells along the z axis, and therefore to the increased dimensionality from the almost ideal 2D case of Sr_2IrO_4. In Figs. 2(b) and 2(c) we show the evolution of the spectra with photon energy, which probes the c-axis dispersion, at the Γ and M points, respectively. The spectra are normalized by the lowest energy peak intensity. The lattice constant in the direction perpendicular to the Ir-O layers, c in Fig. 2(a), is $\sim$20.9 Å. For a tetragonal unit cell, the expected k_z periodicity is $4\pi/c \simeq 0.6$ Å^{-1}. The range shown in Figs. 2(b) and 2(c) covers almost three BZs, with no detectable dispersion comparable with an 80 meV shift of the leading edge at the M point, reported in Ref. [22].

A possible explanation for these seemingly contradictory results is offered by the analysis of Fig. 3(a), which shows as a color plot the k_z dependence of the ARPES signal at the Γ point as in Fig. 2(b), but this time without any normalization, except for that by the photon flux. The spectral weight of the bonding and antibonding bands in a bilayer system is expected to have a markedly different, and in fact nearly opposite, dependence on the excitation energy, due to the opposite reflection symmetry of the states with respect to the intermediate plane between the two layers. We use a simple model, accounting only for the phase difference between the wave functions and considering a free electron final state. For a multilayer system of transverse periodicity d, the k_z dependence of the matrix elements essentially follows a sine wave of period $2\pi/d$, dampened with increasing energy [27]. This behavior has been observed for surface states [28], quantum well states [29], and, more recently, for multilayer graphene [30]. The observed intensity modulation of Fig. 3(a) indeed shows good agreement with the

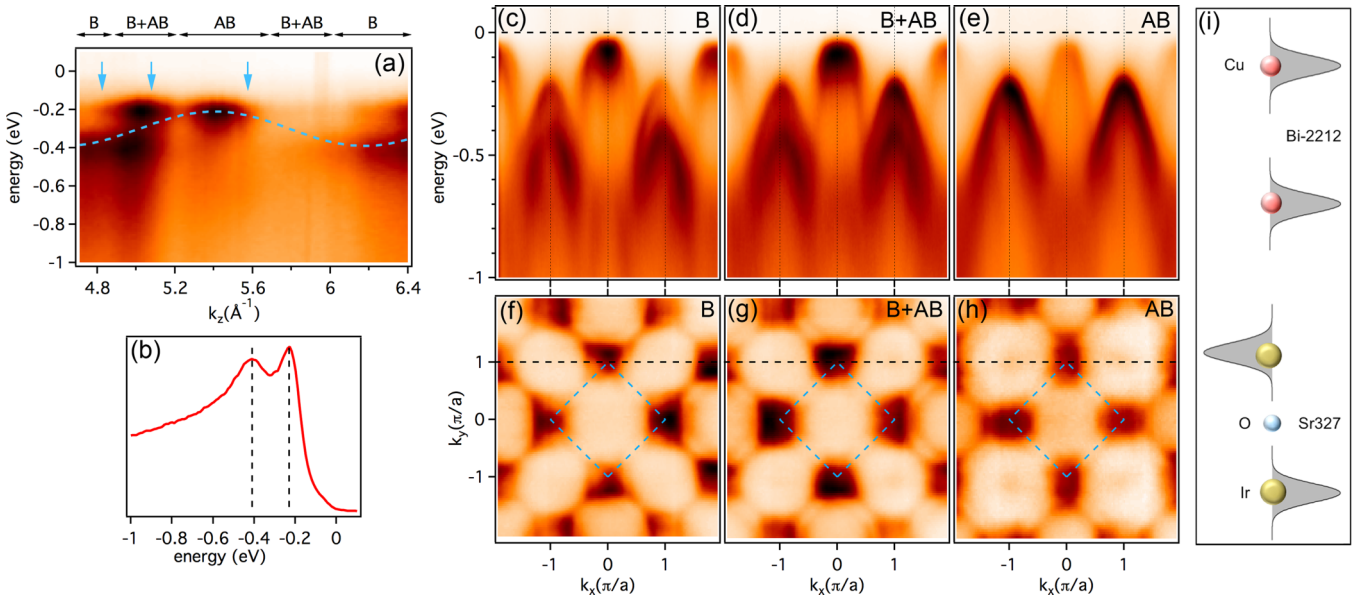

FIG. 3. (Color online) (a) The spectra of Fig. 2(b) are shown as an image plot and with no intensity normalization. The dashed line is a sine wave of period $10\pi/c$. The intervals defined above the panel indicate the approximate ranges where the intensity of either the bonding (B) or antibonding (AB) branch of the $J_{\rm eff} = 3/2$ states is dominant. (b) Energy distribution curve measured at Γ and $h\nu = 96$ eV, in the second BZ. (c)–(e) Band dispersion along a $\Gamma M \Gamma$ line at $k_y = \pi/a$, measured at $h\nu = 85$, 96, and 113 eV, respectively, corresponding to the arrows in (a); the corresponding constant energy cuts at $E = -90$ meV are shown in (f)–(h). In reference to the intervals in (a), (c), (f): B; (d), (g): B + AB; (e), (h): AB. (i) Pictorial representations of the initial state bonding wave functions for Bi-2212 and for $Sr_3Ir_2O_7$.

predictions of this simple approach. In $Sr_3Ir_2O_7$ $d \simeq c/5$, and a sine wave of period $k = 2\pi/(c/5) = 10\pi/c$ (dashed curve) convincingly tracks the transfer of spectral weight between the two branches of the bilayer dispersion.

By choosing the photon energy so that either one or the other of the states are suppressed, the bonding and antibonding bands can almost be mapped separately. Figures 3(c)–3(e) illustrate the dispersion along $\Gamma M \Gamma$ at $k_y = \pi/a$ [dashed lines in panels (f)–(h)], measured for the three photon energies corresponding to the arrows in Fig. 3(a). At the Γ point, the three panels show for the $J_{\rm eff} = 3/2$ states mainly the bonding band (c), both bands with comparable intensity (d), or only the antibonding band (e). The spectrum measured at Γ and $h\nu = 96$ eV, shown in panel (b), clearly shows two peaks, separated by 0.18 eV, corresponding to the bonding and antibonding bands. The distinction is less clear for the $J_{\rm eff} = 1/2$ bands close to M, but signatures of the splitting are visible in panels (f)–(h), which present constant energy cuts at $E = -90$ meV, at the top of the valence band. The corresponding intensity patterns are different, as they map in fact different states. Namely, the rectangular contours at the M points are elongated along different directions in (f) and (h), and are nearly square in (g). Notice that the transfer of spectral weight between the two bands could be misinterpreted as an energy dispersion, which may be the origin of the report of transverse dispersion of Ref. [22].

A further analysis of the intensity modulation of Fig. 3(a) reveals an interesting difference with the related case of the bilayer cuprates. The intensity of the bonding and antibonding bands evolves exactly in antiphase with respect to the case of $Bi_2Sr_2CaCu_2O_{8+\delta}$ (Bi-2212) [27,31]. This is the result of a crucial difference in the structure of the two compounds along the c axis. Namely, a bridging oxygen is present within the bilayer between two Ir ions in $Sr_3Ir_2O_7$, but not in Bi-2212. As a consequence, the wave function of the (bonding) lowest energy state is symmetric in Bi-2212, but antisymmetric in $Sr_3Ir_2O_7$, as shown in the cartoon of Fig. 3(i). In pictorial terms, the oxygen-mediated bond between Ir atoms favors a configuration with an increased $5d$ charge density outside of the bilayer. Since V_0 is evaluated by matching the smooth variation of the photoemission intensity with the expected matrix element modulation, it has a considerable uncertainty which we estimate to be $\sim$5 eV. However, this does not translate into any ambiguity in the assignment of the phase of the wave functions. At these photon energies, an unphysical value of $V_0 > 30$ eV would be needed to translate the data by half a period of the sine wave of Fig. 3(a).

We notice in passing an interesting link between these conclusions and the band structure of $SrIrO_3$, the $n \to \infty$ limit (3D) compound of the series, which remains unavailable. $Sr_3Ir_2O_7$ provides indeed an $n = 2$ sampling of the band structure of $SrIrO_3$. Given the cubic or nearly cubic structure of $SrIrO_3$ the bands are expected to show a similar, holelike, dispersion along the c axis, as they do in the plane. Therefore, the top of the $J_{\rm eff} = 3/2$ manifold is expected at the Γ point, where the (totally symmetric) wave function has the same phase on adjacent layers, and the bottom at Z, where the phase is reversed on each adjacent layer. This is consistent with the previous considerations about the relative energy of the symmetric and antisymmetric states in $Sr_3Ir_2O_7$.

Figure 4(a) presents the measured band dispersion in the second BZ, where the $J_{\rm eff} = 3/2$ intensity is higher, for

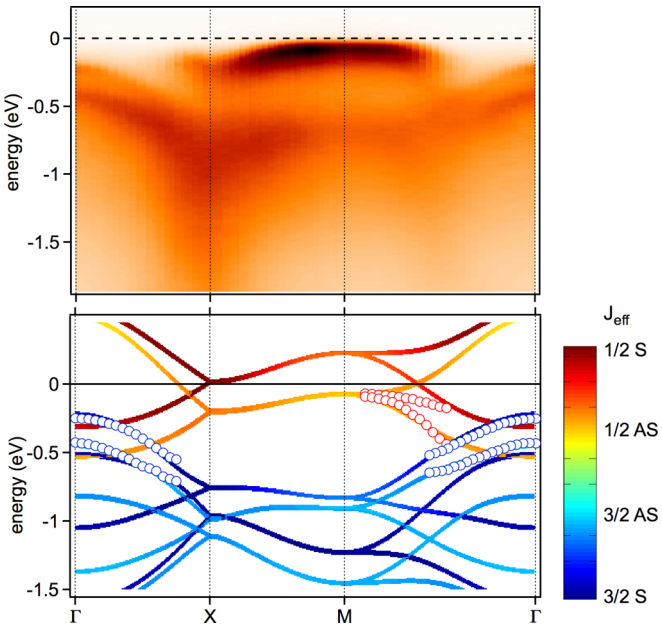

FIG. 4. (Color online) (a) Band dispersion along a $\Gamma X M \Gamma$ path in the second BZ. (b) The peak energies extracted from the experimental data are superposed to the calculated bands of a TB model. The calculation follows Ref. [26], but neglects for simplicity the in-plane octahedra rotation. Colors represent the projected weights of each band on a fourfold bilayer basis set. Intermediate colors indicate mixed character.

$h\nu = 96$ eV, as in Figs. 3(d) and 3(g). Since the line shapes are rather broad, as typical for insulators, for the quantitative analysis of the splitting we used the curvature method, which is known to accurately yield the peak positions [32]. The latter are superimposed in Fig. 4(b) to the result of a tight-binding (TB) model. The calculation is structured as in Ref. [26] and, with respect to our previous work on Ba_2IrO_4 [33], it includes additional interlayer hopping terms, which produce a k-dependent splitting of all bands. The parameters have been slightly adjusted in order to suppress the k offset between the $J_{\rm eff} = 1/2$ band maximum and the M point [26], consistent with the experimental data. More details are available in Ref. [34]. The projected weights of each band on a fourfold bilayer basis set [symmetric (S), antisymmetric (AS); $J_{\rm eff} = 1/2, 3/2$] is encoded in the color scale. For simplicity, we do not consider the staggered tilting of the octahedra and neglect electronic correlations, which are essential to capture hybridization and avoided crossings, and therefore to reproduce the observed energy gap. As a consequence, the results, namely, for the $J_{\rm eff} = 1/2$ manifold, should be considered with caution in the vicinity of the Fermi level. Nevertheless the agreement is excellent further away from E_F.

A comparison of the experimental peak positions with the calculated bands in Fig. 4(b) confirms that the bilayer splitting of the $J_{\rm eff} = 3/2$ states is as large as $\sim$0.2 eV. As a term of comparison, the separation between bonding and antibonding states is only $\sim$0.09 eV in Bi-2212 [27,31]. There, the bilayer splitting is directly related to a relevant interlayer hopping term $t_\perp$, and the energy splitting ΔE is simply $2t_\perp$, at least in a TB approach [35]. In $Sr_3Ir_2O_7$ the t_{2g} states are not orbitally ordered, so that the measured ARPES intensity does not exhibit the dramatic matrix element suppression characteristic of the cuprates. On the other hand, the presence of two interacting states and of comparable energy scales makes the link to the perpendicular hopping term less straightforward [26,36]. What is more important, in $Sr_3Ir_2O_7$ the interlayer hopping is comparable to all other other relevant energy scales, i.e., the in-plane hopping terms [26] and the magnetic exchange terms [5]. Therefore, it cannot be treated as a simple perturbative term to the electronic structure of the monolayer counterpart Sr_2IrO_4.

In summary, a thorough ARPES k-space survey of the electronic structure of the bilayer iridate $Sr_3Ir_2O_7$ reveals a very large splitting of the bonding and antibonding states of mainly $J_{\rm eff} = 3/2$ character. Moreover, the k_z-dependent transfer of spectral weight between these two bands shows that the bonding state has antisymmetric character, opposite to the much studied case of Bi-2212, a typical bilayer cuprate.

L.M. and S.M. equally contributed to this work. We gratefully acknowledge discussions with B. J. Kim, Yeongkwan Kim, and Y. Cao. We acknowledge support by the Swiss NSF, namely, through Grant No. PA00P21-36420 (L.M.) and the Sinergia network on Mott Physics Beyond the Heisenberg Model (MPBH). The Advanced Light Source is supported by the Director, Office of Science, Office of Basic Energy Sciences, of the U.S. Department of Energy under Contract No. DE-AC02-05CH11231. Work in the UK was supported by EPSRC.

[1] B. J. Kim, H. Ohsumi, T. Komesu, S. Sakai, T. Morita, H. Takagi, and T. Arima, Science **323**, 1329 (2009).

[2] B. J. Kim, H. Jin, S. J. Moon, J.-Y. Kim, B.-G. Park, C. S. Leem, J. Yu, T. W. Noh, C. Kim, S.-J. Oh *et al.*, Phys. Rev. Lett. **101**, 076402 (2008).

[3] S. J. Moon, H. Jin, K. W. Kim, W. S. Choi, Y. S. Lee, J. Yu, G. Cao, A. Sumi, H. Funakubo, C. Bernhard *et al.*, Phys. Rev. Lett. **101**, 226402 (2008).

[4] S. Fujiyama, H. Ohsumi, T. Komesu, J. Matsuno, B. J. Kim, M. Takata, T. Arima, and H. Takagi, Phys. Rev. Lett. **108**, 247212 (2012).

[5] J. Kim, A. H. Said, D. Casa, M. H. Upton, T. Gog, M. Daghofer, G. Jackeli, J. van den Brink, G. Khaliullin, and B. J. Kim, Phys. Rev. Lett. **109**, 157402 (2012).

[6] J. Kim, D. Casa, M. H. Upton, T. Gog, Y.-J. Kim, J. F. Mitchell, M. van Veenendaal, M. Daghofer, J. van den Brink, G. Khaliullin *et al.*, Phys. Rev. Lett. **108**, 177003 (2012).

[7] J. W. Kim, Y. Choi, J. Kim, J. F. Mitchell, G. Jackeli, M. Daghofer, J. van den Brink, G. Khaliullin, and B. J. Kim, Phys. Rev. Lett. **109**, 037204 (2012).

[8] S. Boseggia, R. Springell, H. C. Walker, H. M. Rønnow, C. Rüegg, H. Okabe, M. Isobe, R. S. Perry, S. P. Collins, and D. F. McMorrow, Phys. Rev. Lett. **110**, 117207 (2013).
[9] D. Hsieh, F. Mahmood, D. H. Torchinsky, G. Cao, and N. Gedik, Phys. Rev. B **86**, 035128 (2012).
[10] G. Jackeli and G. Khaliullin, Phys. Rev. Lett. **102**, 017205 (2009).
[11] F. Wang and T. Senthil, Phys. Rev. Lett. **106**, 136402 (2011).
[12] H. Watanabe, T. Shirakawa, and S. Yunoki, Phys. Rev. Lett. **105**, 216410 (2010).
[13] C. Martins, M. Aichhorn, L. Vaugier, and S. Biermann, Phys. Rev. Lett. **107**, 266404 (2011).
[14] A. Georges, L. de'Medici, and J. Mravlje, Ann. Rev. Condens. Matter Phys. **4**, 137 (2013).
[15] V. M. Katukuri, H. Stoll, J. van den Brink, and L. Hozoi, Phys. Rev. B **85**, 220402 (2012).
[16] H. Okabe, M. Isobe, E. Takayama-Muromachi, A. Koda, S. Takeshita, M. Hiraishi, M. Miyazaki, R. Kadono, Y. Miyake, and J. Akimitsu, Phys. Rev. B **83**, 155118 (2011).
[17] A. Ino, C. Kim, M. Nakamura, T. Yoshida, T. Mizokawa, Z.-X. Shen, A. Fujimori, T. Kakeshita, H. Eisaki, and S. Uchida, Phys. Rev. B **62**, 4137 (2000).
[18] J. F. Bringley, B. A. Scott, S. J. La Placa, T. R. McGuire, F. Mehran, M. W. McElfresh, and D. E. Cox, Phys. Rev. B **47**, 15269 (1993).
[19] T. Mizokawa, A. Fujimori, H. Namatame, Y. Takeda, and M. Takano, Phys. Rev. B **57**, 9550 (1998).
[20] B. M. Wojek, M. H. Berntsen, S. Boseggia, A. T. Boothroyd, D. Prabhakaran, D. F. McMorrow, H. M. Ronnow, J. Chang, and O. Tjernberg, J. Phys.: Condens. Matter **24**, 415602 (2012).
[21] P. D. C. King, T. Takayama, A. Tamai, E. Rozbicki, S. M. Walker, M. Shi, L. Patthey, R. G. Moore, D. Lu, K. M. Shen *et al.*, Phys. Rev. B **87**, 241106 (2013).
[22] Q. Wang, Y. Cao, J. A. Waugh, S. R. Park, T. F. Qi, O. B. Korneta, G. Cao, and D. S. Dessau, Phys. Rev. B **87**, 245109 (2013).
[23] K. M. Shen, F. Ronning, D. H. Lu, W. S. Lee, N. J. C. Ingle, W. Meevasana, F. Baumberger, A. Damascelli, N. P. Armitage, L. L. Miller *et al.*, Phys. Rev. Lett. **93**, 267002 (2004).
[24] S. Boseggia, R. Springell, H. C. Walker, A. T. Boothroyd, D. Prabhakaran, D. Wermeille, L. Bouchenoire, S. P. Collins, and D. F. McMorrow, Phys. Rev. B **85**, 184432 (2012).
[25] G. Cao, Y. Xin, C. S. Alexander, J. E. Crow, P. Schlottmann, M. K. Crawford, R. L. Harlow, and W. Marshall, Phys. Rev. B **66**, 214412 (2002).
[26] J.-M. Carter and H.-Y. Kee, Phys. Rev. B **87**, 014433 (2013).
[27] D. L. Feng, C. Kim, H. Eisaki, D. H. Lu, A. Damascelli, K. M. Shen, F. Ronning, N. P. Armitage, N. Kaneko, M. Greven *et al.*, Phys. Rev. B **65**, 220501 (2002).
[28] S. G. Louie, P. Thiry, R. Pinchaux, Y. Pétroff, D. Chandesris, and J. Lecante, Phys. Rev. Lett. **44**, 549 (1980).
[29] A. Mugarza, J. E. Ortega, A. Mascaraque, E. G. Michel, K. N. Altmann, and F. J. Himpsel, Phys. Rev. B **62**, 12672 (2000).
[30] T. Ohta, A. Bostwick, J. L. McChesney, T. Seyller, K. Horn, and E. Rotenberg, Phys. Rev. Lett. **98**, 206802 (2007).
[31] A. A. Kordyuk, S. V. Borisenko, T. K. Kim, K. A. Nenkov, M. Knupfer, J. Fink, M. S. Golden, H. Berger, and R. Follath, Phys. Rev. Lett. **89**, 077003 (2002).
[32] P. Zhang, P. Richard, T. Qian, Y.-M. Xu, X. Dai, and H. Ding, Rev. Sci. Instrum. **82**, 043712 (2011).
[33] S. Moser, L. Moreschini, A. Ebrahimi, B. D. Piazza, M. Isobe, H. Okabe, J. Akimitsu, V. V. Mazurenko, K. S. Kim, A. Bostwick *et al.*, New J. Phys. **16**, 013008 (2014).
[34] See Supplemental Material at http://link.aps.org/supplemental/10.1103/PhysRevB.89.201114 for details on the tight-binding model used.
[35] A. I. Liechtenstein, O. Gunnarsson, O. K. Andersen, and R. M. Martin, Phys. Rev. B **54**, 12505 (1996).
[36] Several hopping terms between the two IrO layers affect the band dispersion (five in Ref. [26]). In this qualitative discussion, $t_\perp$ embodies an effective hopping term responsible for the size of the splitting between bonding and antibonding branch.